

Boundary-dependent Self-dualities, Winding Numbers and Asymmetrical Localization in non-Hermitian Quasicrystals

Xiaoming Cai¹

¹*State Key Laboratory of Magnetic Resonance and Atomic and Molecular Physics,
Wuhan Institute of Physics and Mathematics, IAPMST,
Chinese Academy of Sciences, Wuhan 430071, China
(Dated: January 10, 2022)*

We study a non-Hermitian Aubry-André-Harper model with both nonreciprocal hoppings and complex quasiperiodical potentials, which is a typical non-Hermitian quasicrystal. We introduce boundary-dependent self-dualities in this model and obtain analytical results to describe its Asymmetrical Anderson localization and topological phase transitions. We find that the Anderson localization is not necessarily in accordance with the topological phase transitions, which are characteristics of localization of states and topology of energy spectrum respectively. Furthermore, in the localized phase, single-particle states are asymmetrically localized due to non-Hermitian skin effect and have energy-independent localization lengths. We also discuss possible experimental detections of our results in electric circuits.

Introduction.— Anderson localization (AL) has been a fascinating topic in condensed matter physics, ever since the classic work of Anderson in 1958 [1]. In one dimension, it is a known fact that an infinitesimal un-correlated disorder localizes all single-particle states [2]. However, AL phase transitions can exist in one dimensional (1D) quasicrystals, such as the Aubry-André-Harper (AAH) model [3], which has attracted a continuous interest both theoretically and experimentally for the past three decades [4–8]. The system undergoes a sudden AL phase transition at a finite strength of the quasiperiodical potential, which is guaranteed by a self-duality mapping between extended and localized phases. Further searches for generalized self-dualities have been brought to modified AAH models with exact energy-dependent mobility edges [9–12]. Besides AL, the AAH model is also of the topological nature [13, 14] and supports the Thouless pumping [15].

On the other hand, the ability to engineer non-Hermitian Hamiltonians, demonstrated in a series of recent experiments [16–22], sparked a great interest in studying intriguing features and applications of non-Hermitian systems [23–25]. In general, the non-Hermiticity is achieved by introducing nonreciprocal hopping or/and gain and loss, which leads to exotic phenomena, such as parity-time (\mathcal{PT}) phase transitions [26], exceptional points [27, 28], new topological invariants [29, 30], non-Hermitian skin effect and revised bulk-edge correspondence [31–38]. In the presence of disorders, non-Hermitian systems can exhibit unique AL properties, such as purely imaginary disorder induced AL [39–41] and non-Hermitian skin effect induced finite-strength localization-delocalization transition [42–44]. Specifically, non-Hermitian AAH models reveal remarkable impacts of the (quasi)periodical on-site potentials on the \mathcal{PT} symmetry breaking [45–49], butterfly spectrum [46, 50], topological edge states [48–53] and localization properties of eigenstates [49–51, 54–59]. The interplay be-

tween nonreciprocal hopping and (quasi)periodicity gives rise to boundary-dependent topologies [50, 60] and localization properties [61]. Very recently, topological nature of AL phase transition in non-Hermitian AAH models has also come to light [57, 61, 62].

So far, most studies on AL in non-Hermitian AAH models are based on numerical simulations. Few analytical results are available due to the complex nature of energy spectrum. In this Letter, we study topological properties and AL of non-Hermitian quasicrystals by considering a non-Hermitian AAH model with both nonreciprocal hoppings and complex quasiperiodical potentials. We report boundary-dependent self-duality mappings, which is absent so far. We also provide analytical results on topological phase transitions and Asymmetrical AL. The AL phase transition is not necessarily in accordance with the topological phase transitions, which are characteristics of two aspects, localization of states and topology of energy spectrum, respectively. Numerical calculations are also carried out to further confirm these results.

Non-Hermitian Aubry-André-Harper model.— We consider a 1D tight-binding non-Hermitian AAH model described by the following Hamiltonian

$$H = \sum_j [te^{-\eta-i\phi}a_j^\dagger a_{j+1} + te^{\eta+i\phi}a_{j+1}^\dagger a_j + V_j a_j^\dagger a_j], \quad (1)$$

where a_j^\dagger (a_j) is the creation (annihilation) operator of a particle at site j . $t_{L(R)} \equiv te^{\mp\eta}$ is the left(right)-hopping amplitude with η characterizing the asymmetry. ϕ corresponds to an applied magnetic flux or artificial gauge field. $V_j = 2V\cos(2\pi\beta j + \delta - ih)$ is an on-site complex quasiperiodical potential with β an irrational number, e.g., the inverse of the golden ratio $(\sqrt{5}-1)/2$ for infinite systems. For finite systems in numerics, $\beta = F_n/F_{n+1}$ with F_n the n -th Fibonacci number, and the total number of lattice sites $L = F_{n+1}$. Without loss of generality, we will take all parameters to be positive and real. In

the Hermitian limit ($\eta = h = 0$) the system has a self-duality mapping and AL transition occurs at the self-duality symmetry point $V/t = 1$. Extended states for $V/t < 1$ become exponentially localized when $V/t > 1$ with Lyapunov exponents (LEs) $\gamma = \ln(V/t)$ [3], i.e., the inverse of localization lengths. Two limit cases with $\eta = \phi = 0$ and $h = \delta = 0$ were considered in Ref.[61, 62], respectively. In general, non-Hermitian models may suffer from the non-Hermitian skin effect with boundary-dependent spectra and single-particle states [34], and we need to study the properties under different boundaries separately.

Self-duality, topology, and asymmetrical localization under the periodic boundary condition.— Under the periodic boundary condition (PBC), we introduce a duality Fourier transformation

$$\begin{aligned} a_j &= \frac{1}{\sqrt{L}} \sum_{k=1}^L b_k e^{-ik(2\pi\beta j + 2\delta) - 2kh}, \\ a_j^\dagger &= \frac{1}{\sqrt{L}} \sum_{k=1}^L \tilde{b}_k e^{ik(2\pi\beta j + 2\delta) + 2kh}, \end{aligned} \quad (2)$$

where $b_k(\tilde{b}_k)$ is the annihilation (creation) operator in momentum space. It takes the Hamiltonian in real space into momentum space within the same form of Eq.(1), but with simultaneous interchanges $t \leftrightarrow V$, $\eta \leftrightarrow h$ and $\phi \leftrightarrow \delta$, which defines the self-duality [63]. Numerical spectra under PBC support the self-duality and examples are shown in Fig.1(a). An interesting case is obtained in the simultaneous double limit: $t \rightarrow 0$, $\eta \rightarrow \infty$ with $te^\eta \rightarrow t'$ finite, and $V \rightarrow 0$, $h \rightarrow \infty$ with $Ve^h \rightarrow V'$ finite. The Hamiltonian reduces to $H' = \sum_j [t'e^{i\phi} a_{j+1}^\dagger a_j + V'e^{-i(2\pi\beta j + \delta)} a_j^\dagger a_j]$, which is a non-Hermitian half of the classic Hermitian AAH model. The self-duality ensures the transition point $V'/t' = 1$.

Due to connection to the two dimensional quantum Hall system, topological properties of 1D superlattices and quasicrystals in Hermitian [13, 14] and non-Hermitian [57, 61, 62] systems have attracted great interest recently, where some parameter (such as δ or ϕ in our case) is treated as an additional dimension. In the same spirit, here we adopt the winding numbers of energy spectra [57, 61, 62]

$$v_\tau = \lim_{L \rightarrow \infty} \frac{1}{2\pi i} \int_0^{2\pi/L} d\tau \frac{1}{\partial\tau} \log[\det(H)], \quad (3)$$

with $\tau = \phi$ or δ , which refer to the widely used winding numbers evaluated by applying a magnetic flux ϕ and the phase δ in the on-site potential respectively. Analytically derived in the Supplementary Material [63], under the PBC, two winding numbers of energy spectra are related and

$$v_\phi = 1 - v_\delta = \theta\left(\frac{te^\eta}{Ve^h} - 1\right), \quad (4)$$

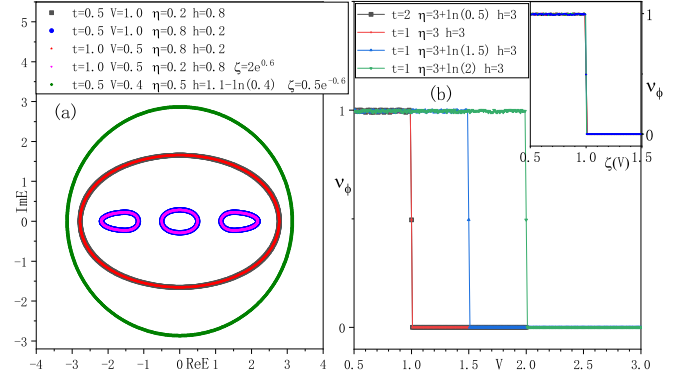


FIG. 1. (Color online) (a) Spectra in the complex energy plane for systems under the periodic boundary condition. (b) Winding number v_ϕ vs V , numerically computed using Eq.(3). Inset in (b): v_ϕ vs $\zeta \equiv Ve^h/te^\eta$, with the transition point $\zeta = 1$. Other parameters: $L = 987$, and $\phi = \delta = 0$.

with $\theta(x)$ the step function. The topological phase transition is also verified by numerical calculations of winding numbers directly using Eq.(3). Examples of numerical v_ϕ vs V are presented in Fig.1(b). After rescaling, all curves collapse with the precise topological phase transition point $\zeta \equiv Ve^h/te^\eta = 1$. Eq.(4) suggests a more general self-duality $\zeta \leftrightarrow 1/\zeta$, which is not supported by numerical results [see Fig.1(a)].

With an irrational β , the quasiperiodical potential acts as a quasirandom disorder which induces the localization of single-particle eigenstates. We denote the right eigenstates of H by $|\Psi_s^R\rangle = \sum_j \psi_s(j) a_j^\dagger |0\rangle$ with s the index of eigenstates. The localization can be characterized by the inverse of the participation ratio (IPR) $P_s = \sum_j |\psi_s(j)|^4 / [\sum_j |\psi_s(j)|^2]^2$. For a localized state the IPR approaches to around 1, whereas for an extended state the IPR is of the order $1/L$. In order to characterize the localization of the system we define the mean inverse of the participation ratio (MIPR) $P = \sum_s P_s / L$. We show MIPRs vs V for different systems under the PBC in Fig.2(a) and corresponding rescaled ones in the inset. All curves collapse with the AL phase transition point $\zeta = 1$, which is the same as the topological phase transition point. No mobility edge is encountered. All eigenstates are extended when $\zeta < 1$, whereas localized when $\zeta > 1$. One can also define (M)IPR for the left eigenstates, which give the same conclusion.

In order to explore details of the localization, in Fig.2(b) we show two typical distributions of right eigenstates in extended and localized phases, respectively. Distinctively, under the PBC the localized state has an asymmetrical exponential decay. We adopt the asym-

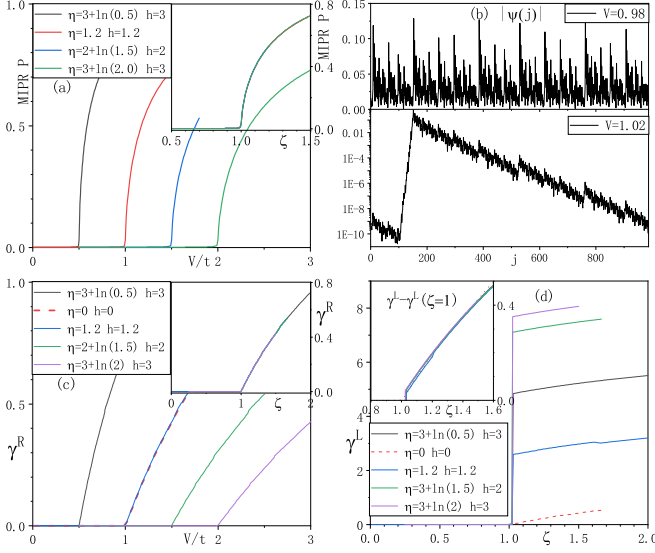


FIG. 2. (Color online) Anderson localization in the non-Hermitian Aubry-André-Harper model under the periodic boundary condition. (a) Mean inverse of the participation ratios (MIPRs) vs V . Inset in (a): Corresponding collapsed MIPRs vs $\zeta \equiv Ve^h/te^\eta$. (b) Two typical distributions $|\psi(j)|$ of right eigenstates for systems in extended and localized phases respectively. $\eta = h = 0.2$, in numerical calculation of (b). (c) Mean right side Lyapunov exponents γ^R , i.e., the inverse of right side localization lengths, vs V . Inset in (c): Corresponding collapsed γ^R vs ζ . (d) Mean left side Lyapunov exponents γ^L vs ζ . Inset in (d): γ^L shifted by the size of jumping. In (c), (d) and insets in them, we also show the Lyapunov exponent for the Hermitian Aubry-André-Harper model (red dash lines). Other parameters: $L = 987$, $t = 1$ and $\phi = \delta = 0$.

metrical wave functions

$$\psi_s(j) \propto \begin{cases} e^{-\gamma_s^R(j-j_0)}, & j > j_0, \\ e^{-\gamma_s^L(j_0-j)}, & j < j_0, \end{cases} \quad (5)$$

which manifest different exponential decaying behaviours on both sides of the localization center j_0 with two LEs $\gamma_s^{R(L)}$. Extracted by fitting the numerical data with Eq.(5), the mean right and left side LEs $\gamma^{R(L)} = \sum_s \gamma_s^{R(L)}/L$ are presented in Fig.2(c)(d), along with the LE for classic Hermitian AAH model. All mean right side LEs γ^R collapse into a single curve with the AL phase transition point $\zeta = 1$. Based on the known LE $\gamma = \ln(V/t)$ for the Hermitian AAH model, the right side LE $\gamma^R = \ln(Ve^h/te^\eta)$ for the non-Hermitian AAH model under the PBC. On the other side, the mean left side LE experiences a sudden jump at $\zeta = 1$. The size of jumping only depends on and approximately equals 2η . After shifting the jump, all mean left side LEs collapse into the LE for Hermitian AAH model, which are shown in the inset of Fig.2(d). Both left and right side LEs are energy-

independent. In a word, under the PBC right eigenstates in the localized phase have LEs $\gamma^R = \ln(Ve^h/te^\eta)$, $\gamma^L = \gamma_0 + \gamma^R$, and $\gamma_0 \simeq 2\eta$.

Skin effect induced novel physics under the open boundary condition.— Under the open boundary condition (OBC), the model with a non-zero η suffers from the non-Hermitian skin effect [29]. In the absence of disorder, all right eigenstates are exponentially localized at the right(left) end when $\eta > (<)0$. In general, we introduce an asymmetric similarity transformation $a_j = e^{(\eta+i\phi)j}b_j$ and $a_j^\dagger = e^{-(\eta+i\phi)j}\tilde{b}_j$. The Hamiltonian Eq.(1) is mapped to

$$H_1 = \sum_j [\tilde{t}b_jb_{j+1} + \tilde{t}b_{j+1}b_j + V_j\tilde{b}_jb_j]. \quad (6)$$

Then Hamiltonians H and H_1 have the exact same spectra and winding numbers $v_{\phi(\delta)}$ under the OBC. Note that here we focus on bulk properties of the system, and these two winding numbers are not useful to predict topological edge states. Please refer to the Supplementary Material for a brief study of edge states [63].

For the moment, we concentrate on the Hamiltonian H_1 , which was originally introduced in Ref.[62] (see also in the Supplementary Material [63]). The model supports a topological AL phase transition at $Ve^h/t = 1$. The winding numbers [63]

$$v_\phi = 0, v_\delta = \theta(Ve^h/t - 1), \quad (7)$$

because H_1 does not depend on ϕ . This model, with $\eta = 0$, does not suffer from the skin effect. All bulk states are extended when $Ve^h/t < 1$. When $Ve^h/t > 1$ all bulk states are exponentially localized with energy-independent and equal right and left side LEs $\gamma_1 = \ln(Ve^h/t)$ [63].

Back to the Hamiltonian H , under the OBC the model does not have a self-duality when $h \neq 0$. When $Ve^h/t < 1$, $v_\delta = 0$, and the spectrum mainly consists of three "bands" without loop. While when $Ve^h/t > 1$, $v_\delta = 1$, and the spectrum consists of loops where the complex spectral trajectory encircles the origin [see Fig.3(a) for examples]. There can not be any self-duality transformation mapping between spectra with different topologies. However, when $h = 0$, based on the relation to the Hermitian AAH model, one can find a self-duality transformation [63]

$$a_j = \frac{1}{\sqrt{L}} e^{i(\phi-\delta)j+\eta j} \sum_k b_k e^{-ik(2\pi\beta j+\delta+\phi)-k\eta}, \\ a_j^\dagger = \frac{1}{\sqrt{L}} e^{-i(\phi-\delta)j-\eta j} \sum_k \tilde{b}_k e^{ik(2\pi\beta j+\delta+\phi)+k\eta}. \quad (8)$$

It interchanges t and V in Hamiltonian $H(h = 0)$. The spectrum of $H(h = 0)$ is the same as for the Hermitian AAH model, with the self-duality critical point $V/t = 1$, which is not the localization critical point [61].

On the other hand, following the asymmetric similarity transformation between H and H_1 , under the OBC a right eigenstate of H satisfies $\psi_s(j) = e^{(\eta+i\phi)j}\psi'_s(j)$ with $\psi'_s(j)$ the corresponding right eigenstate of H_1 . It clearly shows how the skin effect affects states in different phases: For extended states of H_1 , the corresponding wave functions $\psi_s(j)$ are localized at the right end with left side LEs $\gamma^L = \eta$; For localized states of H_1 , wave functions $\psi_s(j)$ have the form

$$\psi_s(j) \propto \begin{cases} e^{-(\gamma_1 - \eta)(j - j_0)}, & j > j_0, \\ e^{-(\gamma_1 + \eta)(j_0 - j)}, & j < j_0. \end{cases} \quad (9)$$

Then the condition $\gamma_1 - \eta > 0$ indicates the localization of right eigenstates, and $\gamma_1 - \eta = 0$ gives the AL phase transition point

$$\zeta \equiv Ve^h/te^\eta = 1. \quad (10)$$

It is the same as the transition point under the PBC, but not the transition point for spectrum or topology under the OBC. Furthermore, in the localized phase, the right and left side LEs

$$\begin{aligned} \gamma^R &= \gamma_1 - \eta = \ln(Ve^h/te^\eta), \\ \gamma^L &= \gamma_1 + \eta = 2\eta + \gamma^R. \end{aligned} \quad (11)$$

The ALs under both boundary conditions are identical, proving the insensitivity of the localized states to boundaries.

The above analytical results are in good agreement with numerical ones. In Fig.3(b) we show MIPRs under the OBC. Due to the skin effect induced boundary-localization nature of right eigenstates, the AL phase transition point should correspond to the most extended case with the smallest MIPR. Therefore, there are deep dives in MIPRs around $\zeta = 1$. In Fig.3(c) we show mean left side LEs which show a jump to 2η at the transition point $\zeta = 1$. When $\zeta < 1$, $\gamma^L = h$ owing to the skin effect, except there is a dive just before the transition point which also indicates the delocalization of states. The dive begins at $Ve^h/t = 1$, which is the topological phase transition point or the AL phase transition point for the model H_1 . This skin effect induced phase was called skin phase [61]. In Fig.3(d) we show mean right side LEs, which show a clear transition at $\zeta = 1$ and correct LEs in localized phase in spite of the unreliable numerical LEs in skin phase due to the right-boundary-localization nature of right eigenstates.

Experimental realization.— The physics of non-Hermitian AAH model [Eq.(1)] can be simulated by electric circuits [57], which recently have turned out to be powerful platforms to simulate non-Hermitian and/or topological phases [64]. The single-particle eigenvalue problem is simulated by the Kirchhoff's current law $I_a = \sum_{b=1}^L J_{ab}V_b$, where J the Laplacian of circuit acts as the effective Hamiltonian, and I_a and V_a are the current and

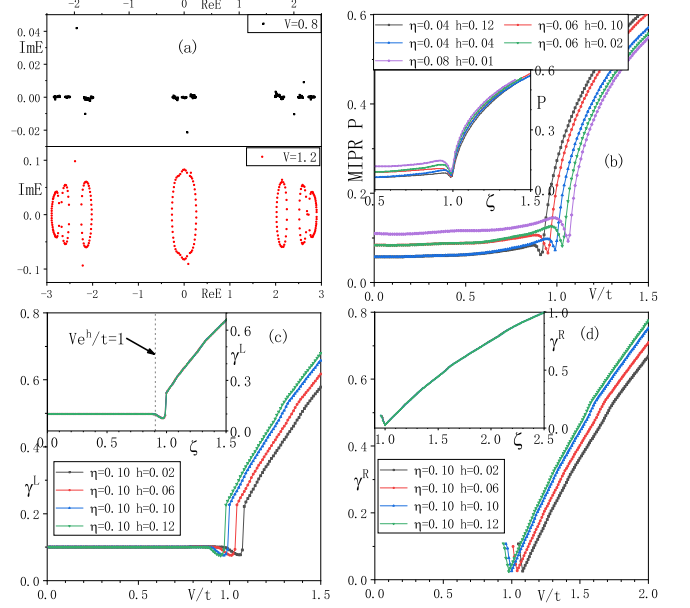


FIG. 3. (Color online) Spectra and Anderson localization for the non-Hermitian Aubry-André-Harper model under the open boundary condition. (a) Two typical spectra in complex energy plane with different winding numbers v_s . $\eta = h = 0.1$, in numerical calculation of (a). (b) Mean inverse of the participation ratios (MIPRs) vs V . Inset in (b): Corresponding MIPRs vs ζ . (c,d) Mean left/right side Lyapunov exponents $\gamma^{L(R)}$ vs V . Insets in (c,d): Corresponding collapsed $\gamma^{L(R)}$ vs ζ . Numerical results before transition points in (d) and inset are not reliable, because of the skin effect induced right-boundary-localization nature of right eigenstates. Other parameters: $L = 233$, $t = 1$ and $\phi = \delta = 0$.

voltage at node a . On-site complex potentials are provided by grounding nodes with proper resistors [65], and asymmetrical hopping amplitudes are realized by negative impedance converters with current inversion (IN-ICs) [66]. Furthermore, the boundary-dependent spectra could be obtained by measuring two-node impedances [50].

In summary, we have analytically studied the non-Hermitian AAH model with both nonreciprocal hoppings and complex quasiperiodical potentials. We first report boundary-dependent self-dualities between localized and extended phases. We also provide analytical results on topological phase transitions and asymmetrical AL. The AL phase transition is not necessarily in accordance with the topological phase transitions, which are characteristics of two aspects, localization of states and topology of energy spectrum, respectively. Under weak disorders, the skin effect dominates and the system exhibits boundary-dependent behaviours. In the localized phase, states are asymmetrically localized with two LEs. Analytical forms of the energy-independent LEs are derived.

We also demonstrate that in non-Hermitian systems the AL is insensitive to boundary conditions. Physics shown above can be experimentally studied in electronic circuits. In the future, it would be interesting to extend the present study to other non-Hermitian quasicrystals, such as the Fibonacci lattice, ladders, and systems with mobility edges.

This work is supported by the NKRDP under Grant No. 2016YFA0301503, the key NSFC grant No. 11534014 No. 11874393 and No. 1167420, and the National Key R&D Program of China No. 2017YFA0304500.

-
- [1] P. W. Anderson, Absence of diffusion in certain random lattices, *Phys. Rev.* **109**, 1492 (1958).
 - [2] Elihu Abrahams, editor. 50 Years of Anderson Localization. World Scientific, 1st edition, 2010.
 - [3] S. Aubry and G. André, Analyticity breaking and Anderson localization in incommensurate lattices, *Ann. Israel. Phys. Soc.* **3**, 133 (1980).
 - [4] M. Kohmoto, Metal-Insulator Transition and Scaling for Incommensurate Systems, *Phys. Rev. Lett.* **51**, 1198(1983).
 - [5] G. Roati, C. D'Errico, L. Fallani, M. Fattori, C. Fort, M. Zaccanti, G. Modugno, M. Modugno, and M. Inguscio, Anderson localization of a non-interacting Bose-Einstein condensate, *Nature (London)* **453**, 895 (2008).
 - [6] X. Cai, L. J. Lang, S. Chen and Y. Wang, Topological superconductor to Anderson localization transition in one-dimensional incommensurate lattices, *Phys. Rev. Lett.* **110**, 176403 (2013).
 - [7] A. Purkayastha, S. Sanyal, A. Dhar, and M. Kulkarni, Anomalous transport in the Aubry-André-Harper model in isolated and open systems, *Phys. Rev. B* **97**, 174206 (2018).
 - [8] M. Rossignolo and L. Dell'Anna, Localization transitions and mobility edges in coupled Aubry-André chains, *Phys. Rev. B* **99**, 054211 (2019).
 - [9] J. Biddle and S. Das Sarma, Predicted mobility edges in one-dimensional incommensurate optical lattices: an exactly solvable model of Anderson localization, *Phys. Rev. Lett.* **104**, 070601 (2010).
 - [10] S. Ganeshan, J. H. Pixley and S. Das Sarma, Nearest neighbor tight binding models with an exact mobility edge in one dimension, *Phys. Rev. Lett.* **114**, 146601 (2015).
 - [11] F. A. An, K. Padavić, E. J. Meier, S. Hegde, S. Ganeshan, J. H. Pixley, S. Vishveshwara and B. Gadway, Observation of tunable mobility edges in generalized Aubry-André lattices, *arXiv:2007.01393*.
 - [12] Y. Wang, X. Xia, L. Zhang, H. Yao, S. Chen, J. You, Q. Zhou, and X. Liu, One dimensional quasiperiodic mosaic lattice with exact mobility edges, *arXiv:2004.11155*.
 - [13] L. Lang, X. Cai, and S. Chen, Edge states and topological phases in one-dimensional optical superlattices, *Phys. Rev. Lett.* **108**, 220401 (2012).
 - [14] S. L. Zhu, Z. D. Wang, Y. H. Chan, and L. M. Duan, Topological Bose-Mott Insulators in a one-dimensional optical superlattice. *Phys. Rev. Lett.* **110**, 075303 (2013).
 - [15] Y. E. Kraus, Y. Lahini, Z. Ringel, M. Verbin and O. Zilberberg, Topological states and adiabatic pumping in quasicrystals, *Phys. Rev. Lett.* **109**, 106402 (2012).
 - [16] J. M. Zeuner, M. C. Rechtsman, Y. Plotnik, Y. Lumer, S. Nolte, M. S. Rudner, M. Segev, and A. Szameit, Observation of a Topological Transition in the Bulk of a Non-Hermitian System, *Phys. Rev. Lett.* **115**, 040402 (2015).
 - [17] C. Poli, M. Bellec, U. Kuhl, F. Mortessagne, and H. Schomerus, Selective enhancement of topologically induced interface states in a dielectric resonator chain, *Nat. Commun.* **6**, 6710 (2015).
 - [18] P. Peng, W. Cao, C. Shen, W. Qu, J. Wen, L. Jiang, and Y. Xiao, Anti-parity-time symmetry with flying atoms, *Nat. Phys.* **12**, 1139 (2016).
 - [19] H. Xu, D. Mason, L. Jiang, and J. G. E. Harris, Topological energy transfer in an optomechanical system with exceptional points, *Nature (London)* **537**, 80 (2016).
 - [20] S. Weimann, M. Kremer, Y. Plotnik, Y. Lumer, S. Nolte, K. G. Makris, M. Segev, M. C. Rechtsman, and A. Szameit, Topologically protected bound states in photonic parity-time-symmetric crystals, *Nat. Mater.* **16**, 433 (2017).
 - [21] M. Pan, H. Zhao, P. Miao, S. Longhi, and L. Feng, Photonic zero mode in a non-Hermitian photonic lattice, *Nat. Commun.* **9**, 1308 (2018).
 - [22] H. Zhou, C. Peng, Y. Yoon, C.W. Hsu, K. A. Nelson, L. Fu, J. D. Joannopoulos, M. Soljačić, and B. Zhen, Observation of bulk fermi arc and polarization half charge from paired exceptional points, *Science* **359**, 1009 (2018).
 - [23] L. Feng, R. El-Ganainy, and L. Ge, Non-Hermitian photonics based on parity-time symmetry, *Nat. Photonics* **11**, 752 (2017).
 - [24] R. El-Ganainy, K. G. Makris, M. Khajavikhan, Z. H. Musslimani, S. Rotter, and D. N. Christodoulides, Non-Hermitian physics and PT symmetry, *Nat. Phys.* **14**, 11 (2018).
 - [25] M. -A. Miri and A. Alù, Exceptional points in optics and photonics, *Science* **363**, eaar7709 (2019).
 - [26] C. M. Bender and S. Boettcher, Real Spectra in Non-Hermitian Hamiltonians Having \mathcal{PT} Symmetry, *Phys. Rev. Lett.* **80**, 5243 (1998).
 - [27] A. Mostafazadeh, Pseudo-Hermitian representation of quantum mechanics, *Int. J. Geom. Meth. Mod. Phys.* **7**, 1191 (2010).
 - [28] M. Znojil, Unitarity corridors to exceptional points, *Phys. Rev. A* **100**, 032124 (2019).
 - [29] Z. Gong, Y. Ashida, K. Kawabata, K. Takasan, S. Higashikawa and M. Ueda, Topological Phases of Non-Hermitian Systems, *Phys. Rev. X* **8**, 031079 (2018).
 - [30] F. Song, S. Yao and Z. Wang, Non-Hermitian Topological Invariants in Real Space, *Phys. Rev. Lett.* **123**, 246801 (2019).
 - [31] T. E. Lee, Anomalous Edge State in a Non-Hermitian Lattice, *Phys. Rev. Lett.* **116**, 133903 (2016).
 - [32] D. Leykam, K. Y. Bliokh, C. Huang, Y. D. Chong, and F. Nori, Edge Modes, Degeneracies, and Topological Numbers in Non-Hermitian Systems, *Phys. Rev. Lett.* **118**, 040401 (2017).
 - [33] H. Shen, B. Zhen, and L. Fu, Topological Band Theory For Non-Hermitian Hamiltonians, *Phys. Rev. Lett.* **120**, 146402 (2018).
 - [34] S. Yao and Z. Wang, Edge States and Topological Invariants of Non-Hermitian Systems, *Phys. Rev. Lett.* **121**, 086803 (2018).
 - [35] F. K. Kunst, E. Edvardsson, J. C. Budich, and E. J.

- Bergholtz, Biorthogonal Bulk-Boundary Correspondence in Non-Hermitian Systems, *Phys. Rev. Lett.* **121**, 026808 (2018).
- [36] K. Yokomizo and S. Murakami, Non-Bloch Band Theory of Non-Hermitian System, *Phys. Rev. Lett.* **123**, 066404 (2019).
- [37] K. Zhang, Z. Yang, and C. Fang, Correspondence between winding numbers and skin modes in non-Hermitian systems, *arXiv:1910.01131*.
- [38] N. Okuma, K. Kawabata, K. Shiozaki, and M. Sato, Topological Origin of Non-Hermitian Skin Effects, *Phys. Rev. Lett.* **124**, 086801 (2020).
- [39] V. Freilikher, M. Pustilnik, and I. Yurkevich, Wave transmission through lossy media in the strong-localization regime, *Phys. Rev. B* **50**, 6017 (1994).
- [40] A. A. Asatryan, N. A. Nicorovici, P. A. Robinson, C. M. de Sterke, and R. C. McPhedran, Electromagnetic localization in one-dimensional stacks with random loss and gain, *Phys. Rev. B* **54**, 3916 (1996).
- [41] A. Basiri, Y. Bromberg, A. Yamilov, H. Cao, and T. Kottos, Light localization induced by a random imaginary refractive index, *Phys. Rev. A* **90**, 043815 (2014).
- [42] N. Hatano and D. R. Nelson, Localization Transitions in Non-Hermitian Quantum Mechanics, *Phys. Rev. Lett.* **77**, 570 (1996).
- [43] P. G. Silvestrov, Vortices in a Superconducting Cylinder: Edge Effects in the Depinned Phase, *Phys. Rev. Lett.* **82**, 3140 (1999).
- [44] S. Longhi, D. Gatti, and G. Della Valle, Robust light transport in non-Hermitian photonic lattices, *Sci. Rep.* **5**, 13376 (2015).
- [45] S. Longhi, \mathcal{PT} -symmetric optical superlattices, *J. Phys. A* **47**, 165302 (2014).
- [46] C. Yuce, \mathcal{PT} -symmetric Aubry-André model, *Phys. Lett. A* **378**, 2024 (2014).
- [47] C. H. Liang, D. D. Scott, and Y. N. Joglekar, \mathcal{PT} restoration via increased loss and gain in \mathcal{PT} -symmetric Aubry-André model, *Phys. Rev. A* **89**, 030102 (2014).
- [48] A. K. Harter, T. E. Lee, and Y. N. Joglekar, \mathcal{PT} -breaking threshold in spatially asymmetric Aubry-André and Harper models: Hidden symmetry and topological states, *Phys. Rev. A* **93**, 062101 (2016).
- [49] N. X. A. Rivolta, H. Benisty, and B. Maes, Topological edge modes with \mathcal{PT} symmetry in a quasiperiodic structure, *Phys. Rev. A* **96**, 023864 (2017).
- [50] Q.-B. Zeng, Y.-B. Yang and Y. Xu, Topological phases in non-Hermitian Aubry-André-Harper models, *Phys. Rev. B* **101**, 020201(R) (2020).
- [51] S. Longhi, Non-Hermitian topological phase transition in \mathcal{PT} -symmetric mode-locked lasers, *Opt. Lett.* **44**, 1190 (2019).
- [52] D. Zhang, L. Tang, L. Lang, H. Yan, and S. Zhu, Non-Hermitian Topological Anderson Insulators, *Sci. China-Phys. Mech. Astron.* **63**, 267062 (2020).
- [53] X. Luo and C. Zhang, Non-Hermitian Disorder-induced Topological insulators, *arXiv:1912.10652*
- [54] S. Longhi, Metal-insulator phase transition in a non-Hermitian Aubry-André-Harper model, *Phys. Rev. B* **100**, 125157 (2019).
- [55] Q.-B. Zeng, S. Chen, and R. Lü, Anderson localization in the non-Hermitian Aubry-André-Harper model with physical gain and loss, *Phys. Rev. A* **95**, 062118 (2017).
- [56] A. Jazaeri and I. I. Satija, Localization transition in incommensurate non-Hermitian systems, *Phys. Rev. E* **63**, 036222 (2001).
- [57] Q.-B. Zeng and Y. Xu, Winding Numbers and Generalized Mobility Edges in Non-Hermitian Systems, *Phys. Rev. Research* **2**, 033052 (2020).
- [58] Y. Liu, X. Jiang, J. Cao, and S. Chen, Non-Hermitian mobility edges in one-dimensional quasicrystals with parity-time symmetry, *Phys. Rev. B* **101**, 174205 (2020).
- [59] T. Liu, H. Guo, Y. Pu, and S. Longhi, Generalized Aubry-André self-duality and mobility edges in non-Hermitian quasiperiodic lattices, *Phys. Rev. B* **102**, 024205 (2020).
- [60] Q.-B. Zeng, Y.-B. Yang and R. Lü, Topological phases in one-dimensional nonreciprocal superlattices, *Phys. Rev. B* **101**, 125418 (2020).
- [61] H. Jiang, L.-J. Lang, C. Yang, S.-L. Zhu, and S. Chen, Interplay of non-Hermitian skin effects and Anderson localization in non-reciprocal quasiperiodic lattices, *Phys. Rev. B* **100**, 054301 (2019).
- [62] S. Longhi, Topological Phase Transition in non-Hermitian Quasicrystals, *Phys. Rev. Lett.* **122**, 237601 (2019).
- [63] See Supplementary Material
- [64] Y. Ashida, Z. Gong, and M. Ueda, Non-Hermitian Physics, *arXiv:2006.01837*.
- [65] J. Schindler, A. Li, M. C. Zheng, F. M. Ellis, and T. Kottos, Experimental study of active *LRC* circuits with \mathcal{PT} symmetries, *Phys. Rev. A* **84**, 040101 (2011).
- [66] T. Hofmann, T. Helbig, C. H. Lee, M. Greiter, and R. Thomale, Chiral Voltage Propagation and Calibration in a Topoelectrical Chern Circuit, *Phys. Rev. Lett.* **122**, 247702 (2019).